Dispersing carbon nanotubes in polymer nanocomposites: detecting individually dispersed tubes

V. Tishkova[*], G. Bonnet[*], P. Puech[*], Ph. Demont[**], E. Flahaut[***], W.S. Bacsa[*]

[*]CEMES-CNRS, 29 Jeanne Marvig, Toulouse 31055, France, wolfgang.bacsa@cemes.fr
[**]LPP, CIRIMAT, UPS, CNRS, Université de Toulouse
[***] LCMIE, CIRIMAT, UPS, CNRS, Université de Toulouse

ABSTRACT

We have performed electrical conductivity measurements and used electron microscopy and Raman spectral mapping as a function of DWNT weight fraction to access the dispersion state. We find that large agglomerates are formed and dispersion depends on loading. Direct current electrical measurements show a percolation at 0.3 wt% of DWNTs and a maximum electrical conductivity of 10^{-2} S/cm are measured at 0.8wt%. The interaction of the outer wall of the DWCNT with the matrix leads to significant change in the Raman G band line shape. Using G band Raman spectral mapping we distinguish regions rich in DWCNTs bundles from regions where DWCNTs are dispersed individually. The presence of large agglomerates in nanocomposites shows that the percolation threshold can be significantly reduced by improving the dispersion of the tubes.

Keywords: nanocomposite, nanotubes, electrical conductivity, TEM, Raman spectroscopy

1 INTRODUCTION

Carbon nanotubes (CNTs) are used to make polymer composites conductive. Small amounts of CNTs (0.1-1 wt%) increase the conductivity by several orders of magnitude. Using thermoplastic polymers as a matrix opens the possibility to combine the unique thermal and solvent resistant properties of the polymer with the electrical properties of CNTs. Poly(ether ether ketone) (PEEK) is a high performance thermoplastic polymer with high thermal and chemical stability as well as excellent mechanical properties [1]. Making PEEK electrically conducting, the composite can be used in antistatic coatings to remove static charges [2] and to shield electromagnetic radiation [3]. Carbon black, carbon nanofibers (CNF), as well as single and multi wall carbon nanotubes (SWNTs and MWNTs) have been incorporated in a PEEK matrix and progress has been achieved by using polyetherimide (PEI) [4] and polysulfones [5]. However, functionalisation has the effect that the thermal and electrical properties are lower compared to the raw SWNTs/PEEK composites [6], [7]. The wrapping or functionalisation of the SWNTs increases the tube-tube electrical resistance. Diez-Pascual et al. [7] measured an electrical conductivity for PEEK/SWNTs composites of 10^{-2} S.cm^{-1} at 1 wt% of nanotube loading and observed percolation at 0.1 wt%. Using multi-wall CNTs (MWNTs) Bangarusampath, et al. [8] has found a percolation threshold in the electrical conductivity for a MWNTs/PEEK composite at 1.3 wt%. The conductivity value of 1 S/cm, required for applications to remove static charges has been achieved at 17 wt% loading [8]. It has been shown that carbon black and graphite fillers have a lower electrical conductivity than CNF. To improve the electric performance of CNT polymer composites it is important to control the filler dispersion in the polymer matrix**.** Comparative analysis of different nanocomposites shows heterogeneity at the experimental percolation threshold depending on the filler polymer and preparation methods [9]. For example the effect of the stirring speed on percolation threshold shows that at lower speed lead to percolation at a lower filling [10].

We have used Raman spectroscopy to characterize the distribution of the carbon nanotubes in the polymer matrix [11]. The Raman shift of the G band can be used to investigate the load-transfer in the nanocomposites [12] and their tensile properties [13], [14].

To learn about the dispersion of nanotubes in a polymer matrix we incorporate DWNTs in PEEK. Double wall carbon nanotubes (DWNTs) can serve as a local sensor for the interaction of the carbon nanotubes with the matrix. It has been shown that doping, pressure and bundling influences the G band of outer and inner tubes [15], [16], [17]. The detetion of the difference in the frequency shifts from individual and bundled DWNTs gives the possibility to distinguish their agglomeration state. We compare the conclusions drawn from from the Raman images with the electrical conductivity measurements. The main advantage of DWNTs compared to SWNTs is that they have an outer tube which can interact with the matrix leaving the inner tube pristine. DWNTs form long bundles favoring the network formation of DWNTs in the polymer matrix.

2 EXPERIMENTAL RESULTS

A drastic increase in the direct current electrical conductivity of DWNTs/PEEK composite takes place when conductive CNTs form a network of connected paths through a insulating PEEK matrix. The conductivity of the composite, σ_{dc}, above the percolation threshold can be modeled with a power law according to percolation theory:

$$\sigma_{dc} = \sigma_0 \, (p - p_c)^t \qquad (1)$$

where σ_0 is the conductivity of the filler, p the filler weight fraction, p_c the percolation threshold (the onset of the insulate-conductor transition) and t is universal critical exponent, which depends on the dimensionality of the conductive network. t=1.6 to 2 in three dimensions and t > 2 have been observed in anisotropic systems.

Electrical conductivity measurements were carried out by recording the complex conductivity $\sigma^*(\omega)$ using a Novocontrol broadband spectrometer. The measurements were carried out in the frequency range of 10^{-2} - 10^6 Hz at room temperature. The real part, $\sigma'(\omega)$ of the complex conductivity $\sigma^*(\omega)$ was investigated. For all the nanocomposite samples considered in this study, the phase lag between the measured impedance and the applied alternating current (ac) voltage was negligible at low frequencies, so that the reported impedance at 0.01 Hz is equivalent to the direct current (dc) resistance with a threshold detection limit of $10^{14}\Omega$. The dc conductivity σ_{dc} of samples was determined from the independent frequency part of $\sigma'(\omega)$ i.e., the low frequency plateau.

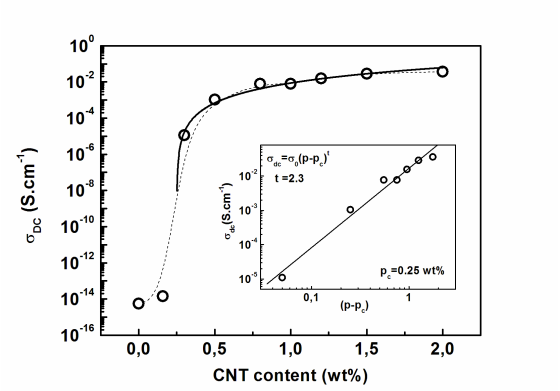

Fig. 1 Electrical conductivity of DW/PEEK composite as a function of tube loading. Percolation is observed at 0.25wt%. The maximum conductivity is $3 \cdot 10^{-2}$ S·cm^{-1}. The inset shows the that the critical exponent is 2.3.

We find that the electrical percolation in DWNTs/PEEK composites occurs when p_c is in the range of 0.2-0.3 wt% as seen in figure 1. A low percolation threshold for a three dimensional isotropic case is expected because the high aspect ratio of DWNTs and their relative good dispersion in the composites. The room temperature maximum conductivity σ_{max} of the composite at 2 wt% of CNTs is about $3 \cdot 10^{-2}$ S·cm^{-1}. Fitting the composite conductivity data with Eq.(1) yields a percolation threshold of 0.25 wt% (solid line in figure 1and inset). The value of exponent t is extracted from the fitting which yields 2.3. This value is close to the theoretical value for the three dimensional conductive network. Extrapolation to p=1 gives $\sigma_0 = 1.7 \cdot 10^{-2}$ S·cm^{-1} which is five orders of magnitude lower than the conductivity measured in sintered DWNTs [19].

It is known that the percolation threshold and the conductivity depend strongly of the polymer type and synthesis method, aspect ratio of CNTs, disentanglement of CNT agglomerates, uniform spatial distribution of individual CNTs and degree of alignment. It is interesting to compare the physical parameters of DWNTs/PEEK composites such as p_c, t and σ_{max} obtained at room temperature with results observed in CNTs /PEEK or CNTs/semi-crystalline matrix (Table I). The same maximum conductivity of 10^{-2} S·cm^{-1} was observed in SWNTs/PEEK composites [6]. In MWNTs/PEEK composites, a percolation was observed at 1.3 wt% with a low value of the critical exponent t = 1.2 and a conductivity of 10^{-2} S·cm^{-1} for 0.2wt% of MWNTs [8]. For a poly(ε-caprolactone)/polylactide semi-crystalline matrix filled by MWNTs, a percolation threshold of 0.2 wt% with a critical exponent of 2.2 and a conductivity of 10^{-4} S·cm^{-1} for 4 wt% were observed [20]. The electrical conductivity of DWNTs/PVDF composites displayed a percolation behavior for only p_c=0.27 wt% of DWNTs and t= 1.91 with a maximum conductivity of 10^{-1} S·cm^{-1} for 2.6 wt% [21].

CNT/polymer	p_c (wt%)	t	p (wt%)	σ (S·cm^{-1})
SWNT/PEEK	0.1		1%	10^{-2}
MWNT/PEEK	1.3	1.2	0.2	10^{-2}
MWNT/PCP	0.2	2.2	4	10^{-4}
DWNT/PVDF	0.27	1.9	2.6	10^{-1}
DWNT/PEEK	0.25	2.3	2.0	$3 \cdot 10^{-2}$

Table 1: CNT composites filling at percolation p_c, critical exponent t and conductivity σ at filling p.

For microscopy, the composites samples were cut into thin (100 nm) slices at room temperature using Ultratome equipped with a diamond knife and deposited on copper TEM grid and we have used a TEM microscope Phillips CM 20 at 150 kV.

Figure 2 shows a TEM image of 0.8wt% DWNTs/PEEK composite. From the image one can see that the DWNTs contain residual catalyst particles (2-20 nm in diameter). The DWNTs diameter is 2-3 nm and the observation of individual nanotubes is found to be challenging due to the presence and thickness of the polymer matrix which reduces the image contrast. The TEM images reveal clearly that most of the nanotubes are in large assemblies and agglomerates.

Raman imaging was carried out using a Horiba T64000 spectrometer at 568 nm excitation wavelength. The sample was placed on a XY mechanical or piezo-electric table (step 3.4 µm). Each Raman spectrum has been fitted with a Lorentzian line function, and then maps of the intensities and positions of the G band are plotted.

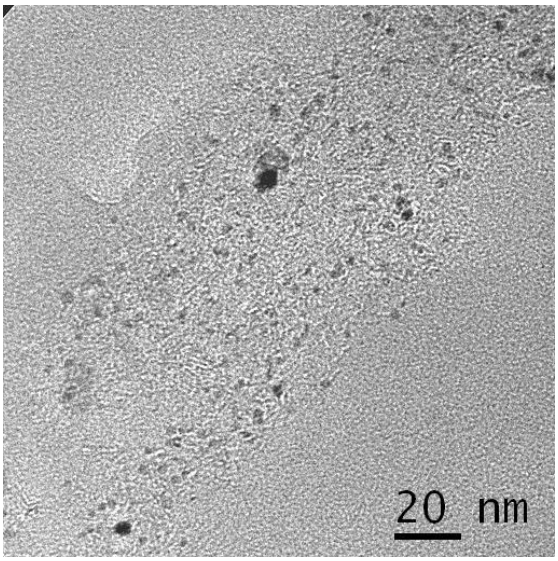

Fig. 2 TEM image of DWNT/PEEK composite (1.5wt%). The tubes density varies at scales of 100 nm. The tubes here are not bundled but entangeled. The dark spots are catalytic metal particles from the DWNT growth.

Figure 3.a-c shows the intensity map of the Raman G band over a larger area (200 by 200 µm) for (a) 0.16 (a), 0.8 (b) and 1.2 wt% (c) (left side). Figure 3.d-f (right side) show the spectral position map of the Raman G band over the same area for the three weight fractions respectively. As a first approximation the intensity I_G of the G band is proportional to the density of tubes. At low concentration the G band is absent in some areas due to the lack of nanotubes.

As the CNTs concentration increases, I_G increases and larger several micrometer sized CNTs agglomerates of nanotubes are visible. Figure 3.d-f show that the G band is located at 1600-1605 cm^{-1} at low CNTs concentration for a large part of the image. At higher concentration the G band is downshifted in energy. At a weight fraction of 1.2 wt% (Fig. 3.f), the G band is strongly downshifted to 1570 cm^{-1} at several positions on the nanocomposite sample.

Figure 3.a-b compares the G band Raman spectra of 0.8 wt % DWNTs/PEEK composite at two different locations of the sample. It has been reported that the G band of DWNTs is composed of two peaks originating from the external and internal tubes [17]. The spectral position of the G band for the outer tubes has been shown to be sensitive to the chemical doping [22] and to external pressure [23]. The splitting is explained by the interaction of the outer tubes with their environment. This means that the interaction of the outer tubes with the polymer matrix can be used as a local sensor for the dispersion of the DWNTs in the PEEK matrix. The splitting of G band indicates that at the probed location the majority of tubes are strongly interacting with the polymer matrix and hence well dispersed. When the G band is observed at the same spectral position as in pristine DWNTs, the tubes are agglomerated. The G band Raman spectrum in figure 4.a is characteristic of DWNTs agglomerates because no splitting was observed.

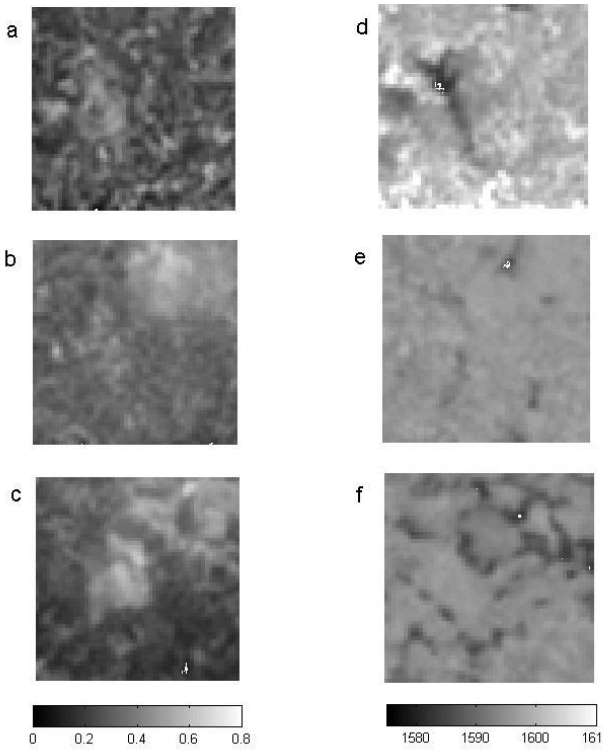

Fig. 3 Spectroscopic image (200 by 200 µm) of the intensity of the Raman G band at three different DW tube fillings 0.16 (a), 0.8 (b) and 1.2 wt% (c) on the left side. On the right side spectroscopic image of the Raman G band in the same area.

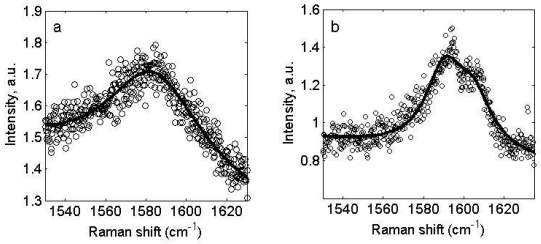

Fig. 4 Raman G band of DWNTs in PEEK at two different locations showing that the band shape varies and can split into two bands due to inner and outer tubes. The splitting only accures when the tubes are strongly interacting with the polymer matrix.

In figure 4.b the upshift of the G band is associated with the interaction between the PEEK matrix and the outer tube and shows that DWNTs are well dispersed in the polymer

matrix. This is in agreement with the observed radial breathing mode (RMB) of DWNTs/PEDOT nanocomposites [24]. RBM band shifts associated with the outer tube diameter was observed in the composite compared to the pristine nanotubes. The position of the RMB band of the inner tube is not affected by the presence of the polymer [24].

3 CONCLUSION

We have used electrical conductivity measurements as a function of CNTs weight fraction and find percolation in the conductivity at filling 0.25wt%. The critical exponent of 2.3 is consistent with a three dimensional percolation network. The electrical conductivity saturates at 1-2 wt% at a value of $3 \cdot 10^{-2}$ $S \cdot cm^{-1}$. TEM of thin 100nm thick slices showed that a large fraction of the tubes is agglomerated or entangled. The Raman G band imaging from DWNTs in the matrix gives the possibility to distinguish regions where the tubes are agglomerated and where the tubes are dispersed individually. The spetroscopic imaging at larger scales (200 µm) shows that only a fraction of the tubes is well dispersed in the polymer matrix.

REFERENCES

[1] Seferis J.C., Polyetheretherketone (PEEK): Processing-structure and properties studies for a matrix in high performance composites. Polymer Composites. 1986, 3(7):158-169.

[2] Markarian J., Increased demands in electronics drive additive developments in conductivity. Plast, Addit Compound. 2005, 1(7) : 26-30.

[3] Li N., Huang Y., Du F., He X., Lin X., Gao H., Ma Y., Li F., Chen Y., Eklund P., Electromagnetic Interference (EMI) Electromagnetic Interference (EMI) Nanotube Epoxy Composites. Nano Lett. 2006, 6 (6) : 1141–1145.

[4] Dıez-Pascual A.M., Naffakh M., Gomez M.A., Marco C., Ellis C., Gonzalez-Domınguez J.M., Anson A., Martınez M.T., Martinez-Rubi Y., Simard B., Ashrafi B., The influence of a compatibilizer on the thermal and dynamic mechanical properties of PEEK/carbon nanotube composites. Nanotechnology. 2009, 315707(20).

[5] Dıez-Pascual A.M., Naffakh M., Gonzalez-Domınguez J.M., Anson A., Martınez-Rubi Y., Martınez M.T., Simard B., Gomez M.A., High performance PEEK/carbon nanotube composites compatibilized with polysulfones-I. Structure and thermal properties. Carbon. 2010, 48 (12) : 3485-3499.

[6] Dıez-Pascual A.M., Naffakh M., Gomez M.A., Marco C., Ellis C., Martınez M.T., Anson A., Gonzalez-Domınguez J.M., Martinez-Rubi Y., Simard B., Development and characterization of PEEK/carbon nanotube composites. Carbon. 2009, 47(13) : 3079-3090.

[7] Dıez-Pascual A.M., Naffakh M., Gonzalez-Domınguez J.M., Anson A., Martınez-Rubi Y., Martınez-Rubi M.T., Simard B., Gomez M.A., Mechanical and electrical properties. Carbon. 2010, 48(12) : 3500-3511.

[8] Bangarusampath D.S., Ruckdäschel H., Altstädt V., Sandler J.K.W., Garray D., Shaffer M.S.P., Chemical Physics Letters. 2009, 482 (1-3) : 105-109.

[9] Bauhofer W., Kovacs J.Z., Composites Science and Technology. 2009, 69 (10) : 1486–1498.

[10] Kovacs J.Z., Velagala B.S., Schulte K., Bauhofer W., Composites Science and Technology. 2007, 67(5) : 922-928.

[11] Zhao Q., Wagner H.D., Phil. Trans. R. Soc. Lond. A., 2004. 362 : 2407–2424.

[12] Wang S., Liang R., Wang B., Zhang C., Chemical Physics Letters. 2008, 457 (4-6): 371–375.

[13] Filiou C., Galiotis C., Composites Science and Technology. 1999, 59(14) : 2149-2161.

[14] Lourie O., Wagner H.D., J. of Materials Research. – 1998, 9(13) : 2418-2422

[15] Puech P., Hubel H., Dunstan D.J., Bassil A., Bacsa R., Peigney A., Flahaut E., Laurent C., Basca W.S., Phys. Stat. Sol. 2004, 241(14) : 3360–3366.

[16] Puech P., Flahaut E., Sapelkin A., Hubel H., Dunstan D. J., Landa G., Bacsa W. S., Phys. Rev. B. 2006, 73, 233408

[17] P. Puech, S. Nanot, B. Raquet, J.-M. Broto, M. Millot, A. W. Anwar, Flahaut E., W. Bacsa, Phys. Status Solidi B. 2010, 1-6, DOI 10.1002/pssb.200945548.

[18] Flahaut E., Bacsa R., Peigney A., Laurent C., Chem. Commun. 2003, 12 : 1442-1443, DOI: 10.1039/b301514a.

[19] Laurent C., Chevallier G., Weibel A., Peigney A., Estournes C., Carbon. 2008, 46 (13) : 1792-1828.

[20] Larendo E., Grimau M., Bello A., Wu D.F., Zhang Y.S., Lin DP., Biomacromolecules. 2010, 11 (5), 1339-1347

[21] Almasri A., Ounaies Z., Kim Y.S., Grunlan J., Macromol. Mater. Eng. 2008, 293 (2) : 123–131

[22] Chen G., Bandow S., Margine E.R., Nisoli C., Kolmogorov A.N., Crespi V.H., Gupta R., Sumanasekera G.U., Iijima S., Eklun P.C., Phys. Rev. Lett. 2003, 90(25)

[23] Puech P., Ghandour A., Sapelkin A., Tinguely C., Flahaut E., Dunstan D. J., Bacsa W., Phys. Rev. B., 2008, 78(4), 045413

[24] Kalbac M., Kavan L., Dunsch L., Composites Science and Technology. 2009, 69(10) : 1553-1557.